THE ASTROPHYSICAL JOURNAL, 366:88–94, 1991 January 1

GINGA OBSERVATIONS OF THREE X-RAY–LUMINOUS EARLY-TYPE GALAXIES: NGC 4472, NGC 4636, AND NGC 3998

H. AWAKI, K. KOYAMA, H. KUNIEDA, S. TAKANO, AND Y. TAWARA
Department of Astrophysics, Nagoya University
AND
T. OHASHI
Department of Physics, University of Tokyo
Received 1989 December 11; accepted 1990 June 25

ABSTRACT

Three X-ray luminous early-type galaxies, NGC 4472, NGC 4636, and NGC 3998, were observed with the *Ginga* satellite. The X-ray spectra of NGC 4472 and NGC 4636 can be described as thermal emission from an optically thin plasma. The temperatures of the hot gas are determined more accurately than with the *Einstein* imaging proportional counter (IPC) observations and are 1.9 ± 0.2 keV and 0.9 ± 0.2 keV for NGC 4472 and NGC 4636, respectively. Assuming hydrostatic equilibrium, the binding masses of NGC 4472 and NGC 4636 are estimated to be $(0.6\text{–}4.6) \times 10^{12}\ M_\odot$ and $(0.5\text{–}2.2) \times 10^{12}\ M_\odot$, respectively.

The X-ray spectrum of NGC 3998 cannot be fitted by a thin thermal model but is well fitted by a power-law model having a photon index of 2.0 ± 0.1, the same sort of spectrum typical of AGNs. Although the X-ray flux of NGC 3998 qualifies it as a low-luminosity Seyfert galaxy, no time variability in less 3×10^4 s could be observed.

Subject headings: galaxies: X-rays — radiation mechanisms — X-rays: spectra

I. INTRODUCTION

About 80 early-type galaxies were observed with the *Einstein Observatory*, and more than half of them were reported to be X-ray sources in the 0.5–4.5 keV band with luminosities ranging from 10^{39} to 10^{42} ergs s^{-1} (Canizares, Fabbiano, and Trinchieri 1987, hereafter CFT). Diffuse X-ray emission extending as far as the optical radii were discovered from most of the X-ray–luminous early-type galaxies (Forman, Jones, and Tucker 1985, hereafter FJT; Trinchieri and Fabbiano 1985, hereafter TF). Using the empirical relationship between X-ray and blue band luminosities in spiral and irregular galaxies (Fabbiano and Trinchieri 1985), the contribution of discrete sources such as X-ray binaries was estimated to be less than 10% for X-ray luminous early-type galaxies (FJT, TF). Their X-ray spectra were consistent with thin thermal emission having a temperature of about 10^7 K (FJT; Trinchieri, Fabbiano, and Canizares 1986, hereafter TFC), which is completely different from those of X-ray binary sources. From these facts, FJT concluded that the X-ray emission from X-ray–luminous early-type galaxies is thermal emission from the hot gaseous halo around the galaxies. The typical gaseous mass and mean density have been estimated to be 10^9–10^{10} $M_\odot$ and about 10^{-3} cm^{-3}, respectively, corresponding to a few percent of the visible mass (FJT, TFC, and CFT).

Assuming that the hot gas is in hydrostatic equilibrium in the galaxy's gravitational potential, FJT estimated that the binding mass of 13 early-type galaxies is about $10^{12}\ M_\odot$. They assumed that the gas temperature was isothermal. However, TFC pointed out that the estimate of the binding mass was subject to an error due to the uncertainty of the gas temperature and its radial gradient. Thus it is essential to determine the gas temperature and radial gradient precisely.

Using the *Ginga* satellite, we attempted to determine the gas temperature more accurately than any previous satellite. For this purpose, we observed two early-type galaxies: NGC 4472 and NGC 4636. These galaxies have been reported to have X-ray emission dominated by hot gas.

The early-type galaxy NGC 3998 was reported to have an active nucleus, because it has a compact nuclear radio source (Condon and Dressel 1978) and shows a broad Hα emission line (Blackman, Wilson, and Ward 1983; Filippenko and Sargent 1985). Using the *Einstein* IPC observation, Dressel and Wilson (1985) reported that the luminosity of NGC 3998 in the 0.5–3.5 keV band was 3×10^{41} ergs s^{-1}, which is consistent with that of low-luminosity AGNs. The X-ray spectrum was reproduced by either thermal emission with a temperature larger than 3 keV or a (nonthermal) power law with photon index of 1–2. Since the spatial resolution (1′) of the IPC was comparable to the optical radius of the galaxy (about 3′), the nuclear source could not be resolved (Dressel and Wilson 1985). In order to distinguish whether the X-ray spectrum of NGC 3998 is thermal or nonthermal, we carried out a broad-band observation with the *Ginga* satellite.

II. OBSERVATIONS

NGC 4472, NGC 4636, and NGC 3998 were observed with the Large Area Counters (LAC; Turner *et al.* 1989) on board the X-ray astronomy satellite *Ginga*. The characteristics of these galaxies are listed in Table 1. The LAC consists of eight identical proportional counters having a total effective area of 4×10^3 cm^2, an energy range of 2–37 keV, and a field of view of $1° \times 2°$ (FWHM). The data were taken with MPC-1 mode, in which X-ray events are accumulated in separate spectra of 48 energy channels from the top and middle layers (Turner *et al.* 1989).

Since the X-ray fluxes of these galaxies were expected to be very faint (less than 1 mCrab), we performed several low-speed linear scans of the LAC field of view over NGC 4636 and NGC

TABLE 1

THREE LUMINOUS GALAXIES

Target	Position[a] (α_{1950}, δ_{1950})	Type[a]	Distance[b] (Mpc)	log ($L_B/L_\odot$)[c]
NGC 4472 (M49) ...	(186°.81, 8°.28)	E1/S0	26	11.32
NGC 4636	(190.07, 2.97)	E0/S0	26	10.81
NGC 3998	(178.18, 55.73)	S0	25	10.55

[a] Sandage and Tammann (RSA).
[b] NGC 4472 and NGC 4636 from CFT, and NGC 3998 from Blackman *et al.* $H_0 = 50$ km s^{-1} Mpc^{-1}.
[c] CFT.

3998. The data were taken with a time resolution of 4 s which corresponds to an angular step of 0°.036. For NGC 4472, we used the data of the Virgo Cluster scan (Takano *et al.* 1989).

For spectral and timing study, we pointed the LAC field of view at the position of each galaxy. The background observations were made at positions offset by 2°.5. These pointing data were taken with a time resolution of 16 s. A log of the scanning and pointing observations is summarized in Table 2.

Since the signal-to-noise ratio in the top layer data is better than the mid-layer (see the Appendix), the data taken from the top layer are used in the following analysis.

III. RESULTS

a) *Scanning Data*

The scan profile of each galaxy in the 1–9 keV band from the top layer is obtained by superposing individual scans. Each profile was fitted with a model of point source plus background (represented as a linear function of position angle). This model gives an acceptable fit. The best-fit values of the source positions and intensities are listed in Table 3. The error regions of the point sources with 90% confidence are given in Figures 1*a*, 1*b*, and 1*c* superposed on the *Einstein* IPC source map (Harris *et al.* 1989).

NGC 4472 is the most luminous IPC source in its error region (Fig. 1*a*). The X-ray fluxes from the other two IPC sources in the same error region are less than 10% of that from NGC 4472 (TFC; Harris *et al.* 1989). Therefore we neglect these possible contaminants from the following analysis.

NGC 4636 is also the most luminous IPC source in its error region (Fig. 1*b*). However, there is another bright IPC source, PG 1241+176, a cataloged QSO. The IPC flux of PG 1241+176 is reported to be about 60% of that of NGC 4636 (TFC, Tananbaum *et al.* 1986; Harris *et al.* 1989). Since the collimator transmission at the position of PG 1241+176 is 30%, we estimate that the contamination of PG 1241+176 is about 20% of the flux of NGC 4636.

TABLE 3

RESULTS OF SCANNING OBSERVATIONS

Target	Energy Band (keV)	Intensity (counts s^{-1})	Position	χ^2 (DOF)
NGC 4472...	1.0–9.0	2.9 ± 0.3	0°.1 ± 0°.1	32.1(21)
	1.0–4.5	2.3 ± 0.2	0.1 (fixed)	41.6(22)
	4.5–9.0	0.6 ± 0.2	0.1 (fixed)	23.8(22)
NGC 4636...	1.0–9.0	2.9 ± 0.7	−0.1 ± 0.1	25.6(20)
	1.0–4.5	2.8 ± 0.5	−0.1 (fixed)	19.1(21)
	4.5–9.0	0.2 ± 0.4	−0.1 (fixed)	25.7(21)
NGC 3998...	1.0–9.0	4.5 ± 0.6	−0.1 ± 0.1	35.4(19)
	1.0–4.5	2.6 ± 0.5	−0.1 (fixed)	26.6(20)
	4.5–9.0	1.9 ± 0.6	−0.1 (fixed)	34.9(20)

NOTE.—Errors of best-fit parameters are at the 90% confidence range.

No IPC source nor any cataloged object is in the error region of NGC 3998 (Fig. 1*c*).

In order to obtain a crude spectral information, we fitted the scan profiles separately in the two energy bands (1–4.5 keV and 4.5–9 keV) with the model described above, but with fixed source positions. In Figure 2, we show the scan profiles of NGC 4636 and the best-fit model profiles. The best intensities are also listed in Table 3. We find that most of the X-ray flux of NGC 4472 and NGC 4636 come from the soft energy band (1.0–4.5 keV). By contrast, the X-ray flux of NGC 3998 in the hard X-ray band (4.5–9 keV) is nearly same as that in the low-energy band (1.0–4.5 keV).

Hayashida *et al.* (1989) analyzed the LAC beam to beam fluctuations of blank X-ray sky at high Galactic latitudes and concluded that the 3 σ level of the source confusion limit in the LAC field of view is 2.6 counts s^{-1} in the 2–10 keV band. The X-ray fluxes of NGC 4472, NGC 4636, and NGC 3998 are comparable to this 3 σ source confusion limit. However, by performing scanning observations, we confirmed that the X-ray fluxes from these galaxies are of a much higher significance level.

b) *Pointing Data*

The X-ray spectra of NGC 4636 and NGC 3998 after subtraction of non–X-ray background (NXB) and cosmic diffuse X-ray background (CXB) are shown in Figures 3*b* and 3*c*. The NXB is deduced using data accumulated while the LAC field of view is occulted by the dark Earth. The spectrum of the CXB is estimated from the mean CXB spectrum observed at high Galactic latitude, and its intensity is estimated from the data of the nearby sky (see Appendix).

Recent *Ginga* observations revealed large-scale intracluster X-ray emission near NGC 4472 due to the Virgo Cluster (Takano *et al.* 1989). Therefore, we also subtracted this emis-

TABLE 2

SUMMARY OF THE X-RAY OBSERVATIONS

	Pointing Observation					
	On-Source		Near Sky			
Target	Date	Exposure $\times 10^3$ (s)	Position (α_{1950}, δ_{1950})	Date	Exposure $\times 10^3$ (s)	Scanning Observation Date
NGC 4472.....	1987 Jun 28	7	(185°.87, 10°.40)	1987 Jun 29	5	1988 Jun 7–8
NGC 4636.....	1988 May 28–29	15	(190.07, 5.67)	1988 May 30	10	1988 May 30
NGC 3998.....	1988 Apr 30–May 1	18	(175.40, 54.29)	1988 May 2	12	1988 May 2

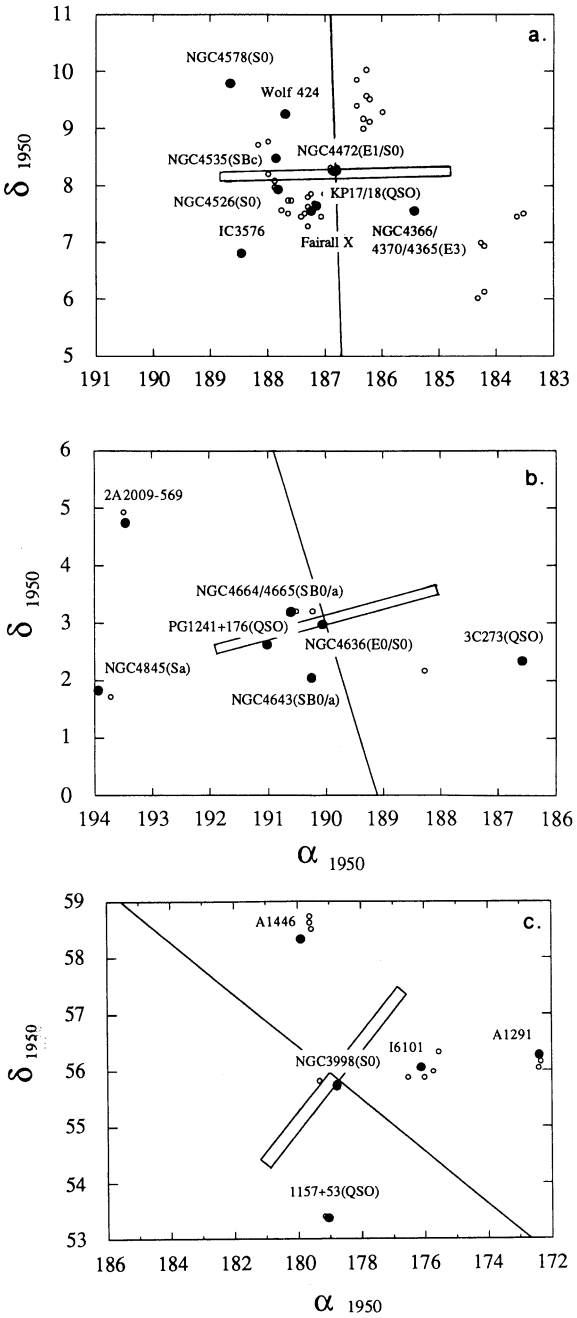

FIG. 1.—X-ray positions and error regions for three galaxies: (*a*) NGC 4472, (*b*) NGC 4636, and (*c*) NGC 3998. The filled and open circles indicate the cataloged X-ray sources and the IPC field sources, respectively. The solid lines show the scan passes. The galaxy types from Sandage and Tammann (RSA) appear in parentheses.

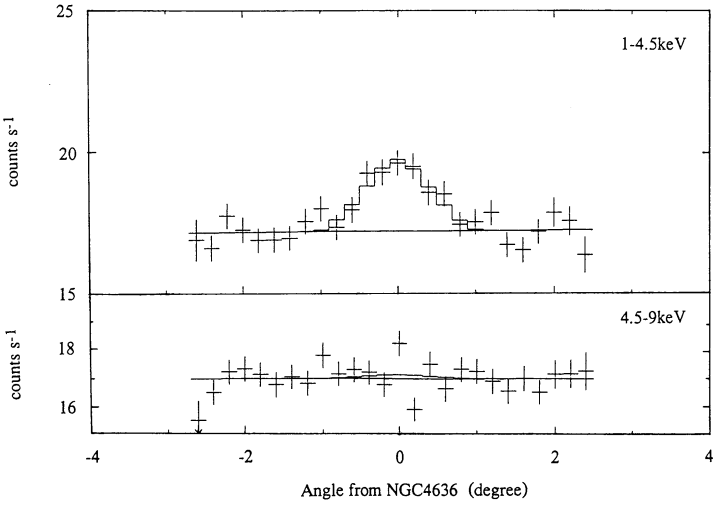

FIG. 2.—Scan profile near NGC 4636 in the 1–4.5 keV band (*upper*) and the 4.5–9.0 keV (*lower*). The histogram shows the best-fit model (BGD + point source).

sion from the on-source data of NGC 4472. The resultant spectrum is shown in Figure 3*a*. We note here that the early report of the X-ray spectrum of NGC 4472 (Koyama 1988) was contamined by the intracluster emission of the Virgo Cluster.

The X-ray intensities of NGC 4472, NGC 4636, and NGC 3998 in the 1–9 keV band are 2.7 ± 0.4, 2.3 ± 0.3, 5.5 ± 0.4 counts s^{-1}, respectively. These values are consistent with the scanning results.

The X-ray emission of NGC 4472 can be fitted by a thin thermal model of solar abundances (Raymond and Smith 1977) with interstellar absorption. The cross section of interstellar absorption is taken from Morrison and McCammon (1983). The normalization factor, temperature, and column density were left as free parameters. The fit was acceptable, with the best-fit temperature of 1.9 ± 0.2 keV.

As is noted in § III*a*, the spectrum of NGC 4636 is possibly contamined by a nearby QSO source, PG 1241+176. A number of QSOs were observed with *Ginga* and are found to have power-law spectra of photon indices between 1.4 and 1.9 (Makino *et al.* 1988). Therefore, the spectrum of NGC 4636 was fitted by a two-component model consisting of a thin thermal spectrum and power law, where the latter component represents the contribution of PG 1241+176. Since there is no published spectrum of PG 1241+176, we fixed the power index at 1.7, a mean value for QSOs observed with *Ginga*. Under this assumption, the temperature of NGC 4636 is determined to be in the range 0.9 ± 0.1 keV. We found that the flux in the 2–10 keV band of PG 1241+176 is about 30% of that of NGC 4636, similar to the result of the IPC observation in the 0.5–4 keV band. We further investigated possible error on the temperature of NGC 4636 caused by an uncertainty of the photon index of PG 1241+176. Allowing the photon index of PG 1241+176 to range from 1.4 to 1.9, we found that the temperature of NGC 4636 is 0.9 ± 0.2 keV.

A thin thermal emission model for the spectrum of NGC 3998 was rejected with a reduced χ^2 value of 2.3 for 19 degrees of freedom. Then we tried nonthermal model fitting and found that a simple model of a power-law spectrum with a photon index of 2.0 ± 0.1 is acceptable.

In Table 4, we summarize the best-fit parameters of NGC 4472, NGC 4636, and NGC 3998.

One might suppose that the contribution of discrete binary X-ray sources in the galaxies may affect the spectral parameters significantly. Therefore we estimate the emission from discrete sources in the following way. The X-ray luminosity of a normal spiral galaxy such as M31 is proportional to the blue band luminosity (Fabbiano and Trinchieri 1985). We apply this relationship to estimate the luminosity from the discrete sources in NGC 4472, NGC 4636, and NGC 3998. The X-ray spectrum of M31 has been observed by *Ginga* (Makishima *et al.* 1989). Fixing this spectral shape and scaling the flux to the

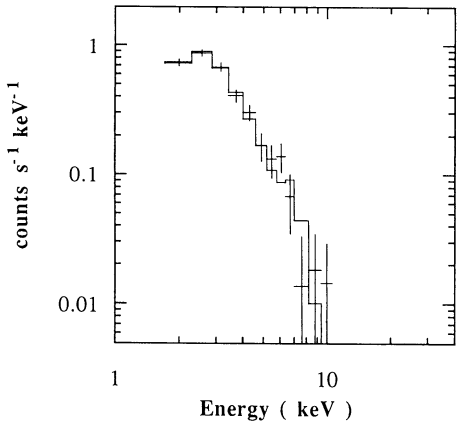

FIG. 3*a*

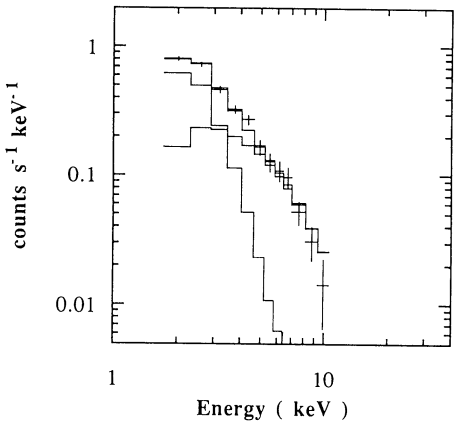

FIG. 3*b*

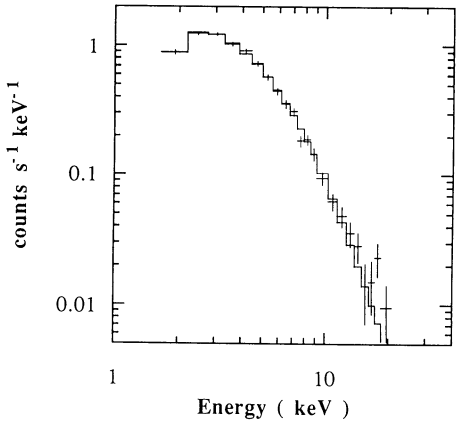

FIG. 3*c*

FIG. 3.—Spectra of three early-type galaxies: (*a*) NGC 4472, (*b*) NGC 4636, and (*c*) NGC 3998. The histogram in each figure shows the best-fit spectral model (thin thermal model of Raymond and Smith 1977 for NGC 4472 and NGC 4636, and power-law model for NGC 3998).

observed blue magnitude, we found that the contributions of the discrete sources to the flux of NGC 4472, NGC 4636, and NGC 3998 in the 2–10 keV band are 8%, 5%, and 3%, respectively. We examined the spectral fitting including these possible contamination of discrete sources and found that the results are not changed significantly from those given in Table 4.

IV. DISCUSSION

a) NGC 4472

The X-ray spectrum of NGC 4472 is well fitted by a thin thermal model with temperature of 1.9 ± 0.2 keV. The extrapolated flux of the best-fit thin thermal model in the 0.2–4.0 keV band is $(1.2 \pm 0.1) \times 10^{-11}$ ergs s^{-1} cm^{-2}, in which we use the $N_{\rm H}$ value of 1.2×10^{21} cm^{-2} (TFC). This is in excellent agreement with the 0.2–4 keV flux of 1.2×10^{-11} ergs s^{-1} cm^{-2} measured by the *Einstein* IPC. Therefore, the thin thermal spectrum observed by *Ginga* in the 2–10 keV band can be smoothly connected to the lower energy band of the *Einstein* IPC. The temperature obtained by *Ginga* provides a more restricted constraint on the temperature than was possible with *Einstein* IPC (TFC).

If the X-ray–emitting gas is in hydrostatic equilibrium, the binding mass of the galaxy can be estimated by the following equation (Fabricant and Gorenstein 1983).

$$M(r) = -\frac{kT(r)}{G\mu m_{\rm H}}\left(\frac{d\log\rho}{d\log r} + \frac{d\log T}{d\log r}\right) r\,,$$

where k, G, T, μ, $m_{\rm H}$, and ρ are Boltzmann's constant, gravitational constant, gas temperature at the radius r, mean molecular weight (taken to be 0.6), the mass of hydrogen atom, and gas density, respectively. $M(r)$ is the mass enclosed within radius r.

Following TFC, we use a gas density gradient ($d\log\rho/d\log r$) of -1.3, an outer radius of the gaseous component of 410″ ($\sim$52 kpc), and a core radius of 5″. The observed temperature ($\langle T\rangle$) is the radiation-weighted gas temperature, which is estimated by assuming a radial temperature gradient $T \propto r^{\alpha}$. As α varies from -0.5 to 0.5 (FJT and CFT), the temperature at the outer radius falls in the range (0.1–1.7) $\langle T\rangle$. Thus, the binding mass of NGC 4472 is estimated to be $(0.6\text{–}4.6) \times 10^{12}\,M_{\odot}$.

b) NGC 4636

The gas temperature of NGC 4636 is found to be 0.9 ± 0.2 keV. The extrapolated flux in the 0.2–4.0 keV band is $(2.8 \pm 1.8) \times 10^{-11}$ ergs s^{-1} cm^{-2} assuming a column density of 1.7×10^{20} cm^{-2} (TFC). The *Einstein* flux in the 0.2–4.0 keV band of 1.2×10^{-11} ergs s^{-1} cm^{-2} (TFC) is within our error range. The *Einstein Observatory* gave an upper limit to the gas temperature of $kT < 1.8$ keV, while the present observation gives finite temperature range of 0.9 ± 0.2 keV.

As in the case of NGC 4472, we estimate the binding mass of $(0.5\text{–}2.2) \times 10^{12}\,M_{\odot}$, where the gas density gradient, the outer radius of the gaseous component, and the core radius are assumed to be -1.5, 360″ ($\sim$32 kpc), and 15″, respectively.

c) NGC 3998

Dressel and Wilson (1985) detected an unresolved IPC source at the center of NGC 3998. The X-ray spectrum was well fitted by a thermal bremsstrahlung as well as a power law model. With the present *Ginga* observation, we exclude the possibility of thermal emission, since the reduced χ^2 of such a model is 2.2 (see Table 4). The X-ray spectrum is fitted by the power-law model with a photon index of 2.0 ± 0.1. The extrapolated flux in the 0.4–3.5 keV band is $(1.6 \pm 0.2) \times 10^{-11}$ ergs s^{-1} cm^{-2}, which is about 3 times larger than the unabsorbed flux of 5.0×10^{-12} ergs s^{-1} cm^{-2} in the same energy band obtained in 1979 (Dressel and Wilson 1985). This flux change over a 9 yr period would be due to

TABLE 4

RESULTS OF X-RAY SPECTRAL FITTING

Target	Flux[a] (ergs s^{-1} cm^{-2})	Lx[a] (ergs s^{-1})	Model	log(N_H)	Temperature (keV) /Photon index	Fe Line[c] (keV)	χ^2(DOF)
NGC 4472.....	5.3×10^{-12}	4×10^{41}	Thermal[b]	<22.0	1.9 ± 0.2	<1.5	7.7(10)
NGC 4636.....	1.6×10^{-12}	1×10^{41}	Thermal[b]	<22.0	0.9 ± 0.2	<40	14.5(12)
NGC 3998.....	1.5×10^{-11}	1×10^{42}	Thermal	<22.0	8.3 ± 0.2	<0.1	42.9(19)
			Power	...	2.0 ± 0.1	...	22.5(19)

NOTE.—Errors bars are 90% confidence.

[a] Energy range is 2–10 keV. Luminosities were estimated at the distance given in Table 1.

[b] Thin thermal model of Raymond and Smith 1977.

[c] Equivalent width.

variability of NGC 3998. Therefore, the scale of the X-ray–emitting region should not be larger than 3 pc. This also exclude the possibility that the X-ray emission is from an extended hot halo.

NGC 3998 has a strong Hα line (Burbidge and Burbidge 1965) and has a broad wing associated with the Hα line (Filippenko and Sargent 1985), similar to the broad lines of Seyfert 1 galaxies. The present determination of a nonthermal power-law spectrum further supports the claim that NGC 3998 has an active galactic nucleus. The X-ray luminosity in the 2–10 keV band is about 1×10^{42} ergs s^{-1} at 25 Mpc (Blackman, Wilson, and Ward 1983). This luminosity is similar to those of low-luminosity Seyfert galaxies such as NGC 4051.

Since rapid variability in the range from 10^3 to 10^4 s has been reported in the X-ray flux of low-luminosity AGNs (Barr and Mushotzky 1986), we searched for rapid variability in NGC 3998. The power spectral density in the 2–10 keV band is found to be comparable to the level of Poisson noise in the frequency range from 10^{-3} to 3×10^{-1} Hz. Searching for longer time scale variations of NGC 3998 using data binned to 512 s, we found no significant intensity variations in the time range from 512 to 4×10^3 s. For example, the 1 σ dispersion of intensities in 4×10^3 s time bins is only 6%, which is extremely small compared to 40% seen in NGC 4051 (H. Kunieda *et al.* 1989, private communication). Apparently, any variability may occur on a longer time scale than can be investigated by our data ($> 3 \times 10^4$ s). If we naively assume the radius of the emitting region to be $R \leq c\Delta t$ and $R \sim 5R_S$, where R_S is the Schwarzschild radius, a longer variability time scale suggests a larger central mass, comparable to the masses of bright AGNs. On the other hand, the low X-ray luminosity of NGC 3998 suggests a smaller accretion rate onto the central object. As one possibility, we may suppose that NGC 3998 is a dormant AGN, which has a smaller accretion rate onto a more massive black hole than a typical low-luminosity Seyfert galaxy. This possibility, of course, should be evaluated by a systematic study of low-luminosity AGNs. NGC 3998 will be one good candidate for this study.

The authors would like to express their thanks to all members of the *Ginga* team, and especially to K. Makishima for valuable comments. Thanks are also due to Professor J. Halpern, J. Turner, M. A. Lim, and K. Leighly for critical reading of the manuscript and comments. The data analysis was performed on the Facom M380 computer of the high energy physics laboratory of Nagoya University. This work was supported in part by the Scientific Research Fund of the Japanese Ministry of Education, Science and Culture under Grant No. 01790168 (S. T.).

APPENDIX

THE METHOD OF BACKGROUND SUBTRACTION

The background events in the LAC arise from the cosmic diffuse X-ray background (CXB) and the non–X-ray background (NXB). We have developed a method to estimate either component based on large amounts of pointing observations of blank sky and the night-time surface of Earth (dark Earth).

I. NON–X-RAY BACKGROUND

The NXB was found to be variable on several time scales. The main sources of time variability are radio activation of the satellite body during a passage through the South Atlantic Anomaly (SAA), cosmic rays, and the charged particles trapped in the geomagnetic field. The variations are parameterized as a function of the satellite orbital condition and the geographic position of the satellite (Awaki 1988; Hayashida *et al.* 1989). We divided the satellite orbits into two types, "high background orbits" (amplitude of variability is 200%–300%), in which the satellite passes through the SAA, and "low background orbits" (amplitude < 20%).

The variation of the NXB in the "high background orbits" is dominated by radio activation with half-lives of about 6 minutes, 41 minutes, and 8 hr (Awaki 1988; Hayashida *et al.* 1989). Shortly after passage through the SAA, the background due to this radioactivity accounts for about 50% of the NXB. Since this background has a constant decay time, we conventionally divided the "high background orbits" into the part "after SAA" passage and the part "before SAA." The part "after SAA" corresponds to the angular satellite position from the ascending node (AA) between $-90°$ and $90°$.

Thus, we divided the satellite orbits into three subgroups. We made three data sets of the NXB corresponding to the three subgroups. The data sets of the NXB were produced using the data when the LAC field of view is occulted by the dark Earth. The

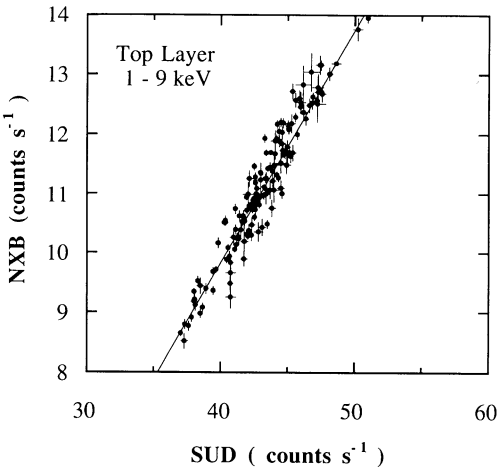

FIG. 4.—The correlation between SUD and NXB in the 1–9 keV band in the top layer in the "low background orbits." The accumulated times of one data point range from 128 s to a few thousand s.

data was collected between 1987 March and 1989 April. We excluded the data from regions of low geomagnetic cut-off rigidity (<9 GeV c^{-1}) and from unusually high background events due to a sudden increase of charged particles. The total accumulation times of the data are 2.6×10^5 s, 8.6×10^4 s, and 7×10^4 s for the "low background orbits," the "after SAA," and the "before SAA," respectively.

We carried out correlation analysis for each data set to search for simple parameters which can reproduce the NXB. We found that the NXB is well reproduced by a linear function of "Surplus Upper Discriminator" (SUD), which is the LAC count rate above 37 keV. Figure 4 shows the correlation between SUD and the 1–9 keV NXB counts in the top layer for the "low background orbits." In this case, the root mean square (rms) scatter of the NXB count rate about the linear fit is 0.3 counts s^{-1}. The rms values of the top and middle layer for each data set are given in Figure 5 and Table 5, where the errors bars are 1 σ ambiguity of the spectrum due to the NXB subtraction. This ambiguity is nearly equal to that of Hayashida *et al.* (1989). One major advantage of the present method is that we can fit the NXB using the single parameter SUD, which ensures good statistics in the fit.

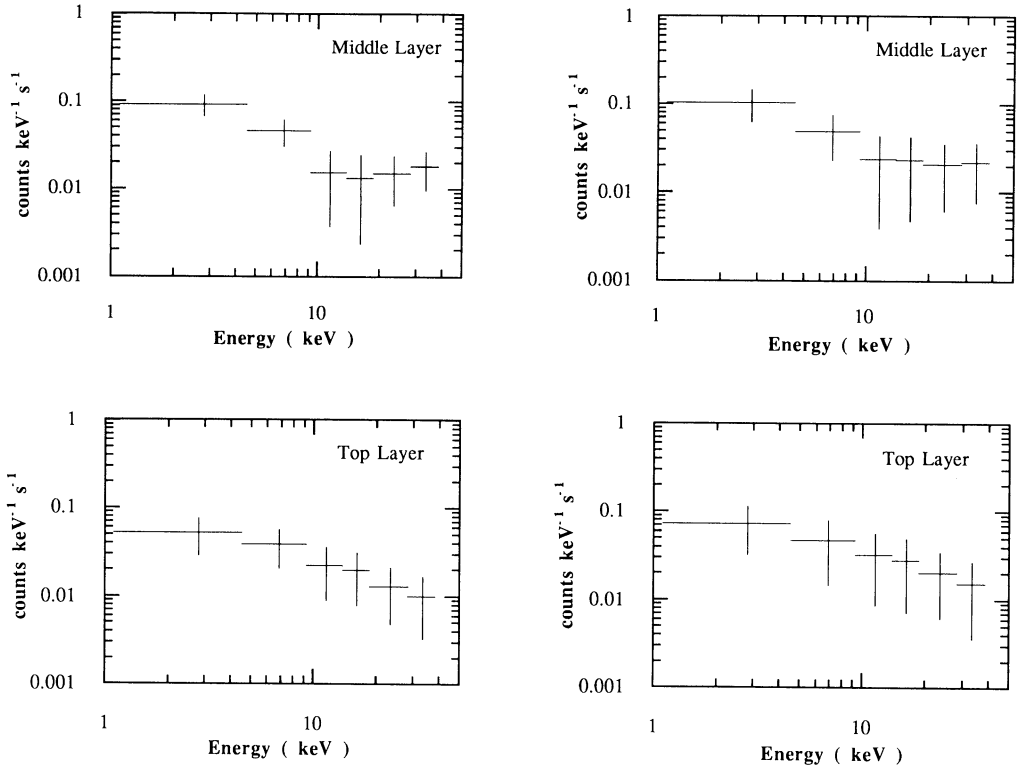

FIG. 5.—Reproducibility of the non–X-ray background at the 1 σ level. The left-hand side gives the reproducibility of the "low background orbits," while the right-hand side is that of the average of the "high background orbits" ("after SAA" and "before SAA").

TABLE 5

REPRODUCIBILITY OF NON–X-RAY BACKGROUND

ENERGY BAND (keV)	LOW BACKGROUND ORBIT		HIGH BACKGROUND ORBIT[a]	
	Middle Layer (counts s^{-1})	Top Layer (counts s^{-1})	Middle Layer (counts s^{-1})	Top Layer (counts s^{-1})
1.1–4.5.....	0.315	0.178	0.353	0.248
4.5–9.2.....	0.215	0.183	0.229	0.220
9.2–13.8.....	0.070	0.103	0.109	0.149
13.8–18.5.....	0.062	0.092	0.110	0.132
18.5–28.2.....	0.145	0.125	0.201	0.196
28.2–38.2.....	0.180	0.100	0.218	0.153

NOTE.—These values include a statistical error.

[a] Averaged values of the high background orbits: "after SAA" and "before SAA."

II. COSMIC X-RAY BACKGROUND

We have examined about 50 blank sky fields at high Galactic latitude ($|b| > 40°$). Here the blank sky was defined as the sky in which the excess counts over mean sky was less than 2 counts s^{-1} ($\sim$0.2 mCrab) in the 2–10 keV range in the top layer. Using the above method for the NXB subtraction, we obtained the spectra from these blank sky regions. The mean count rate of CXB was 14.0 counts s^{-1} in the 2–10 keV band in the top layer with beam-to-beam fluctuation of 0.9 counts s^{-1} (1 σ level). The surface brightness of the mean CXB is 6.3×10^{-8} ergs s^{-1} cm^{-2} sr^{-1} in the 2–10 keV range, or 3.47 keV s^{-1} keV^{-1} cm^{-2} sr^{-1} at 10 keV. This is consistent with the value of 3.2 keV s^{-1} keV^{-1} cm^{-2} sr^{-1} at 10 keV obtained with *HEAO* A-2 experiment (Marshall *et al.* 1980).

We made the mean CXB spectrum by adding about 50 blank sky spectra with total exposure time of 3×10^5 s. A local CXB spectrum for the relevant X-ray source is made from this mean CXB spectrum by normalizing the total flux of the mean spectrum to the observed value of the CXB at locations near the source. This method is justified because no difference in spectral shape among these blank sky data is found although the total flux shows significant deviation. The merit of this method is that it gives better statistics than would the local CXB spectrum obtained in a single blank sky field near the relevant X-ray source.

REFERENCES

Awaki, H. 1988, M. A. thesis, University of Nagoya (in Japanese).
Barr, P., and Mushotzky, R. F. 1986, *Nature*, **320**, 431.
Blackman, C. P., Wilson, A. S., and Ward, M. J. 1983, *M.N.R.A.S.*, **202**, 100.
Burbidge, E. M., and Burbidge, G. R. 1965, *Ap. J.*, **142**, 634.
Canizares, C. R., Fabbiano, G., and Trinchieri, G. 1987, *Ap. J.*, **312**, 503 (CFT).
Condon, J. J., and Dressel, L. L. 1978, *Ap. J.*, **221**, 456.
Dressel, L. L., and Wilson, A. S. 1985, *Ap. J.*, **291**, 668.
Fabbiano, G., and Trinchieri, G. 1985, *Ap. J.*, **296**, 430.
Fabricant, D., and Gorenstein, P. 1983, *Ap. J.*, **267**, 535.
Filippenko, A. V., and Sargent, W. L. W. 1985, *Ap. J. Suppl.*, **57**, 503.
Forman, W., Jones, C., and Tucker, W. 1985, *Ap. J.*, **293**, 102 (FJT).
Harris, D. E., *et al.* 1989, *Version 1, IPC Source List from the Einstein Observatory Source Catalog*, in press.
Hayashida, K., *et al.* 1989, *Pub. Astr. Soc. Japan*, **41**, 373.
Koyama, K. 1988, *Comments Ap.*, **12**, 287.
Makino, F., *et al.* 1988, in *Physics of Neutron Stars and Black Holes*, ed. Y. Tanaka (Tokyo: Universal Academy Press), p. 357.
Makishima, K., *et al.* 1989, *Pub. Astr. Soc. Japan*, **41**, 697.
Marshall, F. E., *et al.* 1980, *Ap. J.*, **235**, 4.
Morrison, M., and McCammon, D. 1983, *Ap. J.*, **270**, 119.
Raymond, J. C., and Smith, B. W. 1977, *Ap. J. Suppl.*, **35**, 419.
Sandage, A., and Tammann, G. 1981, *A Revised Shapley-Ames Catalog of Bright Galaxies* (Washington, D.C.: Carnegie Institution of Washington).
Takano, S., *et al.* 1989, *Nature*, **340**, 289.
Tananbaum, H., Avni, Y., Green, R. F., Schmidt, M., and Zamorani, G. 1986, *Ap. J.*, **305**, 57.
Trinchieri, G., and Fabbiano, G. 1985, *Ap. J.*, **296**, 447 (TF).
Trinchieri, G., Fabbiano, G., and Canizares, C. R. 1986, *Ap. J.*, **310**, 637 (TFC).
Turner, M. J. L., *et al.* 1989, *Pub. Astr. Soc. Japan*, **41**, 345.

H. AWAKI, K. KOYAMA, H. KUNIEDA, S. TAKANO, and Y. TAWARA: Department of Astrophysics, School of Science, Nagoya University, Furo-cho, Chikusa-ku, Nagoya 464-01, Japan

T. OHASHI: Department of Physics, University of Tokyo, 7-3-1, Hongo, Bunkyo-ku, Tokyo 113, Japan